# The Observed Concentration-Mass Relation for Galaxy Clusters

Julia M. Comerford (UC Berkeley) & Priyamvada Natarajan (Yale University)

## Introduction

The properties of clusters of galaxies offer key insights into the assembly process of structure in the universe. Numerical simulations of cosmic structure formation in a hierarchical, dark matter dominated universe suggest that galaxy cluster concentrations, which are a measure of a halo's central density, decrease gradually with virial mass. However, cluster observations have yet to confirm this correlation. Here, we combine new concentration measurements for 10 strong lensing clusters with other measurements in the literature to create the most complete sample of observed cluster concentrations and masses yet assembled. From this sample, we construct an observed concentration-mass relation for galaxy clusters.

## The Observed Concentration-Mass Relation

A halo concentration is defined as the ratio of the halo's virial radius to its scale radius, the radius at which the halo's density profile turns over from ρ~1/r to ρ~1/r³. We define the virial radius as the radius $r_{vir}$ at which the average halo density is $\Delta_{vir}(z)$ times the mean density at the halo redshift z. The resultant halo concentration is $c_{vir}=r_{vir}/r_s$.

We calculate concentrations and virial masses for the 10 lensing clusters fit with NFW profiles in Comerford et al. (2006) and combine these with published X-ray and lensing concentrations from other clusters in the literature. In total, our sample consists of 100 galaxy clusters. Because the distribution of cluster concentrations is so broad, we bin the data into four mass bins with approximately equal numbers of clusters in each bin for a more effective comparison. We determine the mean and standard deviation of the cluster concentrations and masses in each bin, and then fit a power law. Our best-fit power law is

$$c_{vir} = \frac{14.8 \pm 6.1}{1+z}\left(\frac{M_{vir}}{M_0}\right)^{-0.14 \pm 0.12},$$

where the mass normalization is taken to be $M_0 = 1.3 \times 10^{13}\ h^{-1}\ M_{sun}$, as in the simulations. Our best-fit has the same slope and a somewhat larger normalization compared to the Bullock et al. (2001) and Hennawi et al. (2007) concentration-mass relations inferred from dissipationless N-body simulations of ΛCDM cosmic structure formation.

We also note that the concentrations of clusters determined from lensing methods (weak, strong, and a combination of the two) are systematically higher than the concentrations determined by X-ray temperatures. A Kolmogorov-Smirnov test finds only a 28% probability that the lensing and X-ray concentrations are in fact derived from the same parent distribution. The X-ray concentrations may be underpredicted due to deviations from hydrostatic equilibrium, while the lensing concentrations may be overpredicted due to the effects of halo triaxiality and substructure along the line-of-sight.

### Best-fit Power Law to Observed Concentrations and Virial Masses

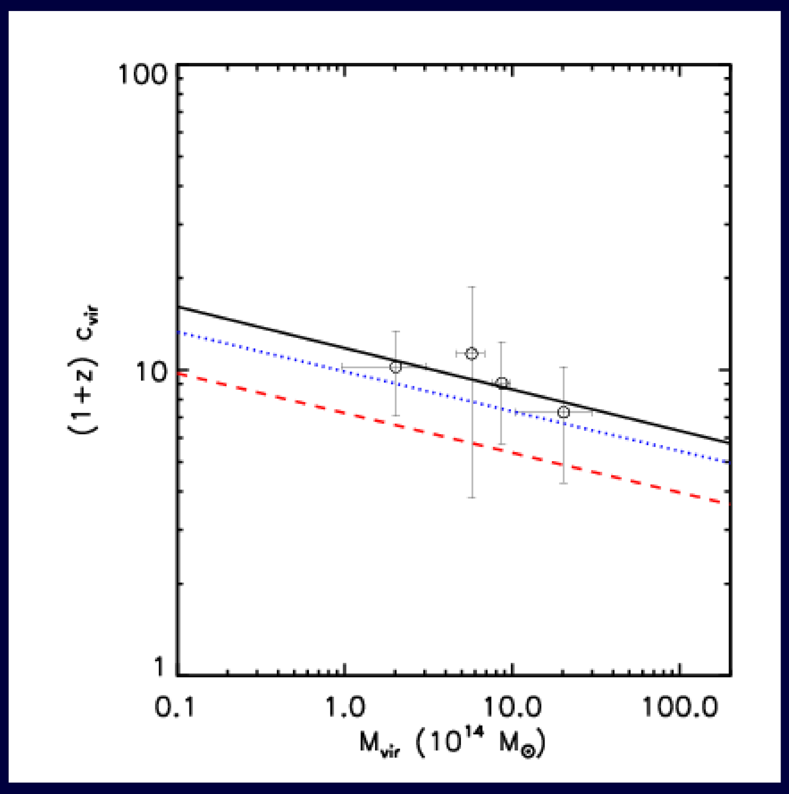


Observed cluster concentrations and virial masses, binned by mass with approximately equal numbers of clusters in each bin. Data points illustrate the mean concentration and mass of each bin, and the solid line is our best fit. The slope of our fit is consistent with fits from simulations, Hennawi et al. (2007) (dotted blue line) and Bullock et al. (2001) (dashed red line), though our normalization is somewhat higher.

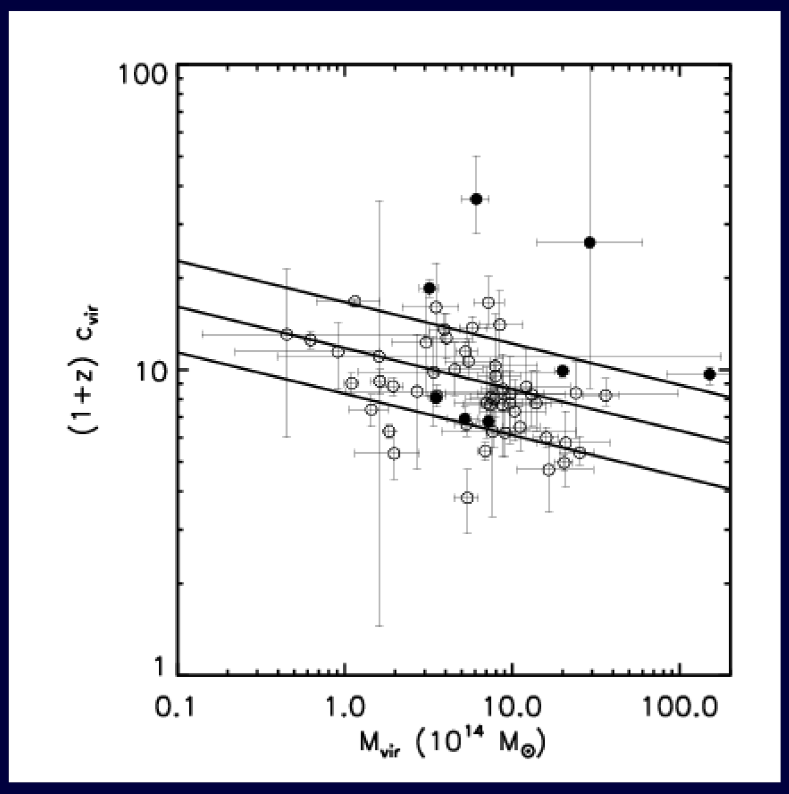


Observed cluster concentrations and virial masses derived from lensing (filled circles) and X-ray (open circles) measurements. For reference, the solids lines depict the best-fit power law to our complete sample and its 1-σ scatter. The lensing concentrations appear systematically higher than the X-ray concentrations, and a Kolmogorov-Smirnov test confirms that the lensing results likely belong to a different distribution.

### Concentrations for Fixed Halo Mass

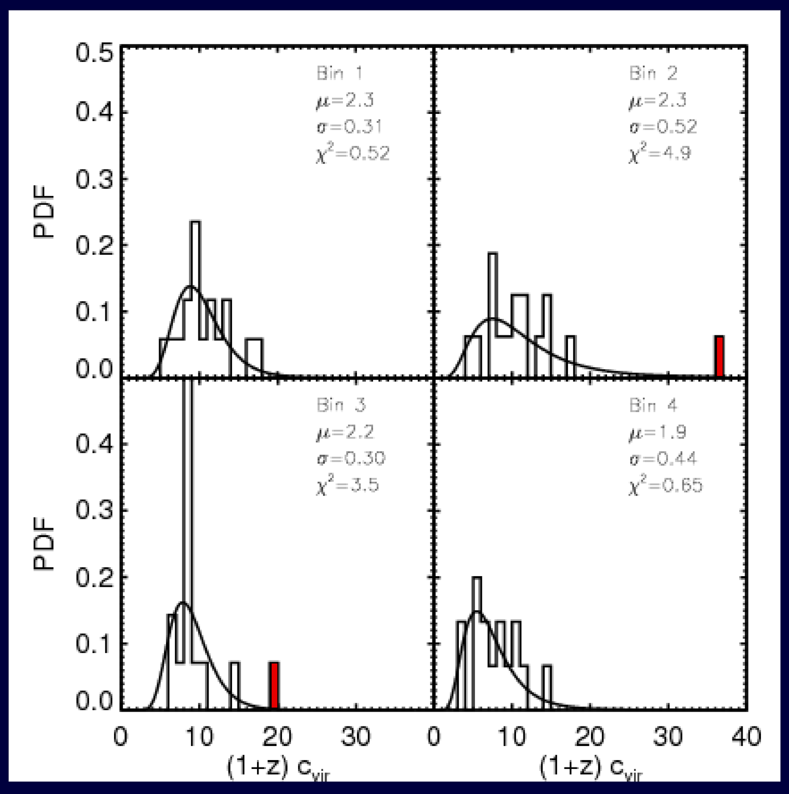


Log-normal fits to normalized histograms of observed cluster concentrations, binned by mass. The mass ranges are $M_{vir} < 4 \times 10^{14}\ M_{sun}$, $4 \times 10^{14}\ M_{sun} < M_{vir} < 7.3 \times 10^{14}\ M_{sun}$, $7.3 \times 10^{14}\ M_{sun} < M_{vir} < 12 \times 10^{14}\ M_{sun}$, and $M_{vir} > 12 \times 10^{14}\ M_{sun}$ for bin 1 to bin 4, respectively. For each mass bin the expectation value μ, standard deviation σ, and $\chi^2$ of the best-fit log-normal function are also given.

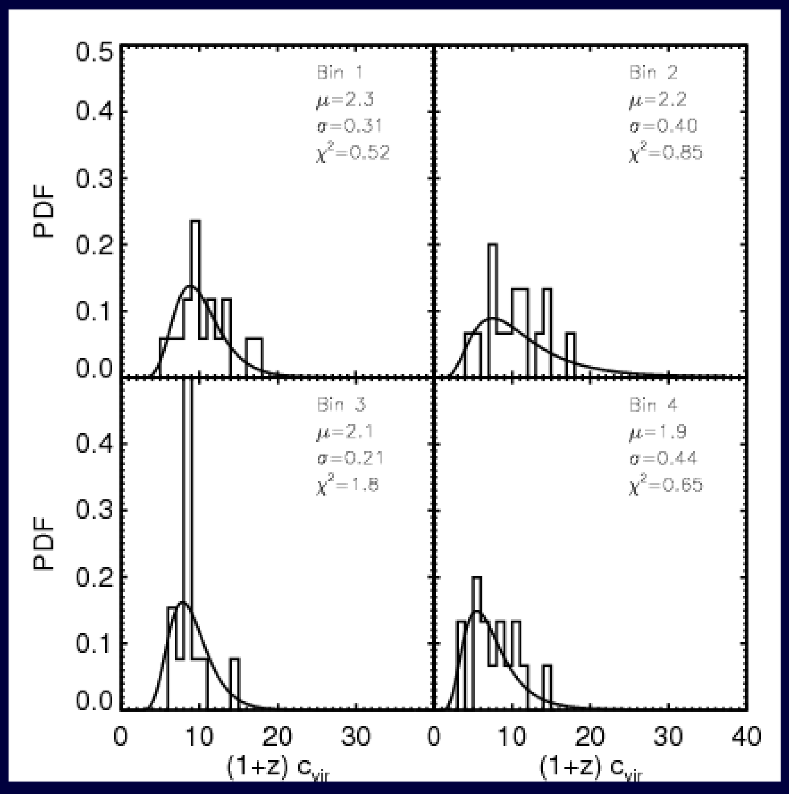


As in the figure on the left, but with concentrations greater than 2-σ from the expectation value omitted. This excluded the highest concentration cluster in bin 2 and in bin 3. The resultant fits improved by up to a factor of 6 in $\chi^2$.

### New Cluster Concentrations and Masses Determined via Strong Lensing

| Cluster | Lens[a] | $c_{200}$ | $M_{200}$ ($10^{14} M_\odot$) | $c_{vir}$ | $M_{vir}$ ($10^{14} M_\odot$) |
|---|---|---|---|---|---|
| ClG 2244−02 | | 4.3 ± 0.4 | 4.5 ± 0.9 | 5.2 ± 0.5 | 5.2 ± 1.1 |
| Abell 370 | G1 | 4.8 ± 0.2 | 9.0 ± 1.0 | 5.8 ± 0.3 | 10. ± 1 |
| | G2 | 5.2 ± 0.3 | 6.7 ± 0.7 | 6.3 ± 0.3 | 7.7 ± 0.8 |
| 3C 220.1 | | 4.3 ± 0.2 | 3.1 ± 0.3 | 5.0 ± 0.2 | 3.5 ± 0.3 |
| MS 2137.3−2353 | | 13 ± 1 | 2.9 ± 0.4 | 16 ± 1 | 3.2 ± 0.4 |
| MS 0451.6−0305 | | 5.5 ± 0.3 | 18 ± 2 | 6.4 ± 0.3 | 20. ± 2 |
| MS 1137.5+6625 | | 3.3 ± 0.2 | 6.5 ± 0.7 | 3.8 ± 0.2 | 7.2 ± 0.8 |
| ClG 0054−27[b] | G1 | 1.2 ± 0.1 | 0.42 ± 0.07 | 1.5 ± 0.1 | 0.52 ± 0.09 |
| | G2 | 2.1 ± 0.1 | 0.95 ± 0.12 | 2.5 ± 0.1 | 1.1 ± 0.1 |
| Cl 0016+1609[b] | DG 256 | 2.1 ± 0.1 | 1.1 ± 0.2 | 2.5 ± 0.1 | 1.3 ± 0.2 |
| | DG 251 | 2.3 ± 0.1 | 0.51 ± 0.06 | 2.7 ± 0.1 | 0.59 ± 0.07 |
| | DG 224 | 3.1 ± 0.2 | 3.1 ± 0.4 | 3.6 ± 0.2 | 3.6 ± 0.4 |
| Cl 0939+4713 | G1 | 4.5 ± 0.3 | 0.71 ± 0.11 | 5.4 ± 0.4 | 0.81 ± 0.12 |
| | G2 | 3.7 ± 0.3 | 1.1 ± 0.2 | 4.5 ± 0.3 | 1.2 ± 0.2 |
| | G3 | 4.5 ± 0.2 | 1.4 ± 0.1 | 5.4 ± 0.3 | 1.6 ± 0.2 |
| ZwCl 0024+1652 | #362 | 4.6 ± 0.2 | 3.1 ± 0.1 | 5.5 ± 0.3 | 2.6 ± 0.3 |
| | #374 | 4.3 ± 0.2 | 3.7 ± 0.5 | 5.1 ± 0.3 | 4.2 ± 0.5 |
| | #380 | 3.4 ± 0.2 | 2.7 ± 0.3 | 4.1 ± 0.2 | 3.2 ± 0.3 |

[a]See Comerford et al. (2006) for lens identification.

[b]Because these cluster arcs have no published redshifts, we calculate the concentration and mass assuming $D_s/D_{ls}=1$. Note that we do not use these concentration and mass determinations in our observed concentration-mass fit.

## Anomalously High Concentration Clusters

Numerical simulations suggest that concentrations for fixed halo mass are log-normally distributed. To test this hypothesis for observed clusters, we group the clusters into four mass bins and fit a log-normal function to the distribution of concentrations in each bin. The observed concentrations appear to be consistent with a log-normal distribution, with the exception of a couple of high concentration clusters that lie beyond the tail of the distribution To determine how well the bulk of concentrations, without the outliers, is fit by a log-normal distribution, we omit all concentrations greater than 2-σ from the expectation value. The resultant fits improved so that all four bins are well-fit by a log-normal function.

The two outliers are Cl 0024 and MS 2137, clusters that, along with Abell 1689, are well-known for their anomalously high concentrations. However, recent papers have suggested that the high concentration measurements may be explained by physical effects. For example, Cl 0024 exhibits prominent substructure that may account for its high concentration estimates (Kneib et al. 2003). Also, the high lensing concentration of MS 2137 may be explained by an elongated halo with its major axis close to the line of sight (Gavazzi 2005). Finally, the concentration of Abell 1689 has come down to a consensus of $c_{vir}$ ~ 6 – 8 (Limousin et al. 2006) due to careful, detailed modeling including an unprecedented large number of strong lensing constraints.

## Conclusions

We have presented a comprehensive set of observed galaxy cluster concentrations and virial masses, including new concentration estimates for 10 strong lensing clusters. With this data, we fit the dependence of the concentration parameter with virial mass to a power law to compare with the relation obtained in simulations. The main results of this analysis are:

- The observed cluster concentrations and virial masses are best fit by a power law with a slope consistent with the value of -0.13 found by simulations, in contrast to previous observational studies which found a steeper slope or no slope at all. The normalization of our best fit is at least 20% higher than the normalizations found by simulations. We suspect that adiabatic contraction and a steepening of the dark matter density profile in response to the collapse of baryons in real clusters offers a likely explanation for this systematic offset.

- Cluster concentrations derived from lensing analyses are systematically higher than concentrations derived via X-ray temperatures. We find that observed strong lensing clusters have concentrations 55% higher, on average, than the rest of the cluster population, a larger factor than found in simulations. The discrepancy between lensing and X-ray concentrations is likely due to some combination of X-ray concentrations underpredicted for unrelaxed clusters and lensing concentrations overpredicted due to halo triaxiality and structure along the line of sight.

- For fixed mass, the majority of observed clusters are distributed log-normally in concentration, with a few exceptions. The log-normal distribution is predicted by simulations, but has not been measured observationally prior to this work. The exceptions to this log-normal distribution are two clusters well-known for their anomalously high concentration measurements.

- The three clusters with the highest concentration measurements have been well studied, and the physical effects (such as halo elongation and substructure) behind these large concentrations are better understood. These effects need to be accounted for with careful modeling.

Although our observed concentration-mass relation for galaxy clusters is reasonably consistent (albeit with a higher normalization) with present simulations, the Millennium simulation will offer the best comparison set to the observed relation reported here. This simulation will offer ample statistics spanning all four mass bins for a direct comparison with our data.

### Anomalously High Concentration Measurements

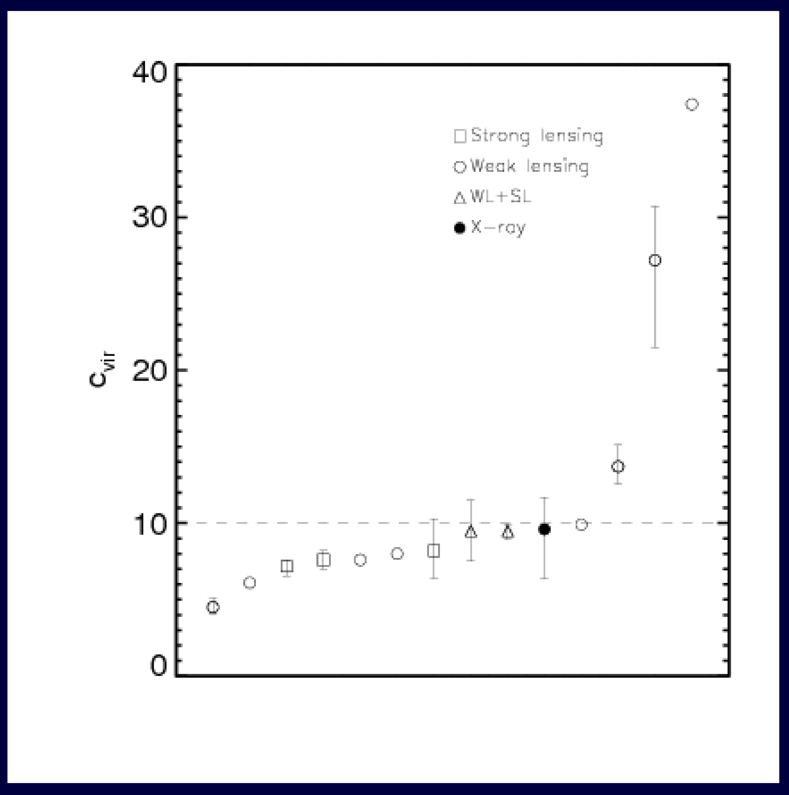


Observed concentrations for the cluster Abell 1689, ordered from lowest to highest. Only weak lensing measurements produce the anomalously high $c_{vir}$ > 10 concentrations (dashed line).

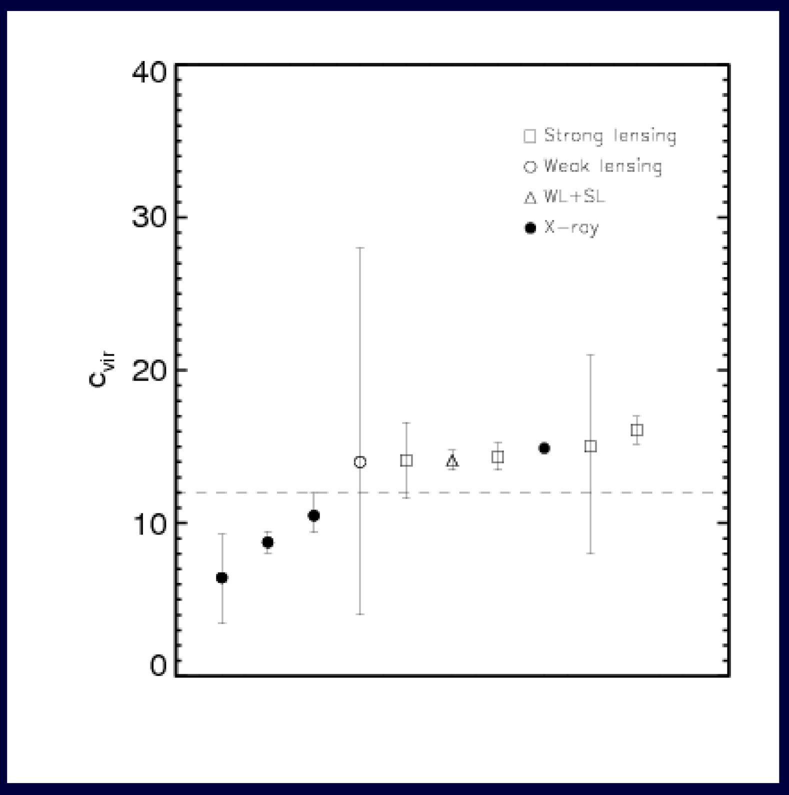


Observed concentrations for the cluster MS 2137, ordered from lowest to highest. Note that all of the smaller values of concentration $c_{vir}$ < 12 (dashed line), which are more consistent with predictions from observed and simulated c-M relations, are from X-ray measurements.

**Acknowledgements**: J.M.C. and P.N. acknowledge insightful and useful discussions with Matthias Bartelmann. We also benefited from exchanges at the concentration discussion group at the KITP workshop on applications of gravitational lensing. J.M.C. acknowledges support by a National Science Foundation Graduate Research Fellowship.

**References:**
Bullock, J. et al. 2001, MNRAS, 321, 559
Comerford, J.M. et al. 2006, ApJ, 642, 39
Gavazzi, R. 2005, A&A, 443, 793
Hennawi, J.F. et al. 2007, ApJ, 654, 714
Kneib, J. et al. 2003, ApJ, 598, 804
Limousin, M. et al. 2006, astro-ph/0612165

**See Comerford & Natarajan 2007, MNRAS, submitted (astro-ph/0703126) for more details.**